ISSN 0006-2979, Biochemistry (Moscow), 2015, Vol. 80, No. 4, pp. 424-432. © Pleiades Publishing, Ltd., 2015.
Published in Russian in Biokhimiya, 2015, Vol. 80, No. 4, pp. 497-507.
Originally published in Biochemistry (Moscow) On-Line Papers in Press, as Manuscript BM14-235, February 15, 2015.

pH Might Play a Role in Regulating the Function of Paired Amphipathic Helices Domains of Human Sin3B by Altering Structure and Thermodynamic Stability

Tauheed Hasan[#], Mashook Ali[#], Daman Saluja, and Laishram Rajendrakumar Singh*

Dr. B. R. Ambedkar Center for Biomedical Research, University of Delhi, Delhi-110-007, India;
fax: +91-11-2766-6248; E-mail: lairksingh@gmail.com; directoracbr@gmail.com; director@acbr.du.ac.in

Received August 19, 2014
Revision received September 29, 2014

Abstract—Human Sin3B (hSin3B), a transcription regulator, is a scaffold protein that binds to different transcription factors and regulates transcription. It consists of six conserved domains that include four paired amphipathic helices (PAH 1-4), histone deacetylase interaction domain (HID), and highly conserved region (HCR). Interestingly, the PAH domains of hSin3B are significantly homologous to each other, yet each one interacts with a specific set of unique transcription factors. Though various partners interacting with hSin3B PAH domains have been characterized, there is no structural information available on the individual PAH domains of hSin3B. Here we characterize the structure and stability of different PAH domains of hSin3B at both nuclear and physiological pH values by using different optical probes. We found that the native state structure and stability of different PAH domains are different at nuclear pH where hSin3B performs its biological function. We also found that PAH2 and PAH3 behave differently at both nuclear and physiological pH in terms of native state structure and thermodynamic stability, while the structural identity of PAH1 remains unaltered at both pH values. The study indicates that the structural heterogeneity of different PAH domains might be responsible for having a unique set of interacting transcription factors.

DOI: 10.1134/S0006297915040057

Key words: protein structure, thermodynamic stability, circular dichroism, transcription regulator, scaffold protein

Sin3, a global transcription regulator, helps to regulate many biological functions including nucleosome remodeling, DNA methylation, cell proliferation, and apoptosis [1, 2]. Sin3 does not bind to DNA but is a scaffold protein that helps the transcription of various genes by interacting with different transcription factors, forming Sin3 complex. The core complex of Sin3 consists of eight components in humans: SIN3, HDAC1, HDAC2, RbAp46, RbAp48, SAP30, SAP18, and SDS3 [3, 4]. Sin3 has six distinct conserved domains that include four repeats of paired amphipathic helices (PAH1-4), histone deacetylase interaction domain (HID), and the highly conserved region (HCR) [1]. There is a high degree of similarity between PAH1 and PAH2 of Sin3 in various organisms, but PAH3 domains share relatively low levels of sequence identity with the PAH1 and PAH2 domains (25 and 16%, respectively), yet these PAH domains recognize different sequence motifs, thereby exhibiting high degree of specificity for their targets [5, 6]. In humans, two isoforms of Sin3 are present (hSin3A and hSin3B) that are encoded by two separate genes that are considered to be the result of gene duplication [7]. Human Sin3A and Sin3B proteins are approximately 57% identical throughout the length of their polypeptide chains with the highest degree of homology localized in the PAH and HID regions [8, 9].

The PAH domains of hSin3B are responsible for interacting with different transcription factors [10-12]. Various interacting partners of PAH1, PAH2, and PAH3 have been identified in humans, and these are responsible for carrying out different biological functions [13]. Some data are also available in the literature about the structural and functional aspects of the PAH domains [2, 14]. In addition, atomic level structural information on Sin3 is available in the literature, but most of the structural studies have been carried out on the PAH domains of mouse or other species than human [6, 14-17]. Therefore, lack of

Abbreviations: HCR, highly conserved region; HID, histone deacetylase interaction domain; PAH, paired amphipathic helices domain.

[#] These authors contributed equally to this work.

* To whom correspondence should be addressed.

structural information about the different PAH domains of humans impedes systematic analysis with data coming from interaction studies. Here we report investigation of the differences in the structure and stability of different PAH domains of human Sin3B at nuclear pH (6.3-6.8) and physiological pH (7.0) using various spectroscopic tools. We found that there is subtle variation in the structure of the PAH domains of hSin3B at nuclear pH where Sin3 performs its biological functions. We also found that PAH2 and PAH3 behave differently at both the nuclear and physiological pH in terms of native state structure and stability, while the structural identity of PAH1 remains unaltered at both pH values. Our study suggests that the difference in the conformation of native state structure or structural flexibility of the PAH domains might be responsible for interacting with specific binding partners.

MATERIALS AND METHODS

Cloning, expression, and purification of proteins. The human fetal brain cDNA library was amplified according to the instruction of the supplier (Clontech Laboratory Inc., USA) and used for PCR amplification of various PAH domains of hSin3B using primers for PAH1 (5′-AGCTGCGGATCCACGTAGAAGACG-3′ and 5′-TCTAGTCTCGAGCCGAGGGGAAGAAAAG-3′), PAH2 (5′-CATAGGGGATCCTGGAGTCCGATTC-3′ and 5′-GTGCATCTCGAGCGGCCCGTTTCCTGT-3′), and PAH3 (5′-CAGTGGGGATCCACGGGACTCTGCAG-3′ and 5′-ATGGAACTCGAGAAGGACAGCTCTTTTACC-3′) with a *Bam*HI restriction site in the forward primer and *Xho*I in reverse primer. The PCR amplified product was ligated to TA vector (Promega, USA) and then subcloned into pGEX-5x3 expression vectors using the restriction sites. The ligation product was transformed into *E. coli* DH5α competent cells and grown overnight on a Luria–Bertani (LB) agar plate containing ampicillin (100 μg/ml). A recombinant clone for each PAH domain was subjected to DNA sequencing to confirm the reading frame and sequence. For purification of the PAH domain, the plasmids were transformed into *E. coli* BL21(DE3) competent cells, and a single colony was grown overnight in LB medium containing 100 μg/ml ampicillin at 37°C with shaking at 250-300 rpm [18]. Fresh culture (1 liter) was inoculated with 10 ml of the overnight culture, and it was vigorously agitated for 3-4 h at 250 rpm until the OD_{600} reached 0.5-0.6. Overexpression of PAH domains was induced with 0.5 mM isopropyl-β-D-1-thiogalactopyranoside (IPTG) at 37°C with vigorous agitation for 4 h before harvesting the cells by centrifugation at 8000*g* for 20 min at 4°C. The cell pellet was frozen and stored at –80°C and used within one week.

Cells were lysed in buffer containing 50 mM Tris (pH 8.0) (MP Biomedicals, USA), 250 mM NaCl (G-Biosciences, USA), 0.1% NP-40 (Sigma, USA), and 1% bacterial protease inhibitor cocktail (Sigma). The cells were lysed by giving six cycles of sonication at 60% efficiency. The bacterial lysate was centrifuged at 8000*g* for 20 min at 4°C to remove the insoluble fraction. Supernatant (4 ml) was mixed with 2 ml bed volume of glutathione-Sepharose (GE Healthcare, USA) and incubated for 30 min at 4°C with gentle shaking. The glutathione-Sepharose was washed five times with 10 ml of phosphate buffered saline (140 mM NaCl, 2.7 mM KCl, 10 mM Na_2HPO_4, and 1.8 mM KH_2PO_4). Approximately 4 mg of the fusion protein was incubated with 40 μl of Factor Xa enzyme (1 μg/μl) (GE Healthcare) at 22°C for 16 h in 4 ml of cleavage buffer (50 mM Tris, pH 8.0, 150 mM NaCl, and 1 mM $CaCl_2$) to cleave the GST tag from the fusion protein. The suspension was centrifuged at 500*g* for 5 min to pellet the resin. The supernatant contains the purified protein and Factor Xa. Factor Xa was removed from the protein using a HiTrap Benzamidine FF (high sub) column (GE Healthcare). This column captures the Factor Xa, thus enabling the collection of pure protease-free protein in the eluate. Protein solutions were dialyzed extensively against 0.1 M KCl at pH 7.0 in the cold (4°C) to remove the salts and then lyophilized for later experiments.

Thermal denaturation studies. Thermal denaturation of the protein was studied using a Jasco J-810 spectropolarimeter equipped with a Peltier-type temperature controller at heating rate of 1°C/min. This scan rate was found to provide adequate time for equilibration. Each sample was heated from 20 to 85°C. The change in absorbance with increasing temperature was followed at 222 nm. About 500 data points of each transition curve were collected. Measurements were repeated at least three times. After denaturation, the protein sample was immediately cooled to measure reversibility of the reaction. Each heat-induced transition curve was analyzed for T_m (midpoint of denaturation) and ΔH_m (enthalpy change at T_m) using a nonlinear least squares method according to the relation:

$$y(T) = \frac{y_N(T) + y_D(T)\exp[-\Delta H_m/R(1/T - 1/T_m)]}{1 + \exp[-\Delta H_m/R(1/T - 1/T_m)]}, \quad (1)$$

where $y(T)$ is the optical property at temperature T (K); $y_N(T)$ and $y_D(T)$ are the optical properties of the native and denatured protein molecules at T (K), respectively; and R is the gas constant. In the analysis of the transition curve, it was assumed that a parabolic function describes the dependence of the optical properties of the native and denatured protein molecules (i.e. $y_N(T) = a_N + b_N T + c_N T^2$ and $y_D(T) = a_D + b_D T + c_D T^2$, where a_N, b_N, c_N, a_D, b_D, and c_D are temperature-independent coefficients). A plot of ΔH_m versus T_m at each pH gave the value of ΔC_p, the change in heat capacity at constant pressure. The value of Gibbs free energy change at any temperature T, $\Delta G_D(T)$, was estimated using the Gibbs–Helmholtz equation (Eq. (2)) with values of ΔH_m, T_m, and ΔC_p:

$$\Delta G_D(T) = \Delta H_m(T_m - T) - \Delta C_p[(T_m - T) + \mathrm{In}T(T/T_m)]. \quad (2)$$

Circular dichroism (CD) measurements. CD measurements were made using a Jasco J-810 spectropolarimeter equipped with a Peltier-type temperature controller with six accumulations. Protein concentration used for the far UV CD measurements was 0.6 mg/ml. A cell of 0.1-cm pathlength was used for the measurements. The protein samples were preincubated overnight at the desired solvent conditions. The necessary blank was subtracted from each measurement. All readings were made at 25°C. The CD instrument was routinely calibrated with D-10-camphorsulfonic acid.

Intrinsic fluorescence measurements. Fluorescence spectra of the protein samples were measured in a Perkin Elmer LS 55 spectrofluorimeter in a 3-mm quartz cell with both excitation and emission slits set at 10 nm. Protein concentration for all the experiments was 10 μM. For intrinsic fluorescence measurements, the excitation wavelength was 268 nm, while the emission spectra were recorded from 290-400 nm at 25°C. All measured spectra have been subtracted for the contribution of blanks. For the 1-anilino-8-naphthalene sulfonate (ANS) binding experiments, the excitation wavelength was 360 nm, and emission spectra were recorded from 400 to 600 nm. ANS concentration was kept at 16-fold that of the protein concentration. The concentration of ANS was determined experimentally using ε, the molar absorption coefficient value of 5000 $M^{-1}\cdot cm^{-1}$ at 350 nm [19, 20] and was filtered before use to remove insoluble particles. Spectra were recorded in a 5-mm quartz cell at 25°C with excitation and emission slits of 10 nm at scanning speed of 100 nm/min in a Perkin-Elmer LS-55 spectroluminometer. Blanks were subtracted against corresponding samples.

RESULTS

To investigate the possibility for differences in the thermodynamic stability of PAH domains, we first performed heat-induced denaturation of the proteins at different pH values (6.3, 6.5, 6.8, and 7.0) by following changes at θ_{222}, the difference in CD signal at wavelength 222 nm, for all the three PAH proteins. We chose these pH values as the pH of the nucleus is slightly below 7.0 but higher than 6.0. In this study, pH 7.0 represents the optimum physiological pH condition. All denaturation curves were reversible. Figure 1 shows heat-induced denaturation profiles of PAH1, PAH2, and PAH3 at different pH values. Each denaturation curve of a protein at a given pH was analyzed for ΔH_m and T_m using a nonlinear least squares method that involves fitting the entire data of the transition curve to Eq. (1) with all eight free parameters (a_N, b_N, c_N, a_D, b_D, c_D, ΔH_m, and T_m). The thermodynamic parameters (ΔH_m and T_m) for all the three proteins obtained at different pH values are given in Table 1. Values of ΔC_p of the proteins were determined by plotting ΔH_m and T_m values generated at the different pH values. The values of ΔC_p evaluated in this manner were 1.53 and 1.54, respectively, for PAH2 and PAH3 (see Table 1). We could not evaluate the ΔC_p of PAH1, as there was no significant change in the ΔH_m and T_m values with change in pH. Since the estimated ΔC_p values of PAH2 and PAH3 were identical, we used the same ΔC_p for the estimation of ΔG_D^o of PAH1. Values of ΔG_D^o (the value of ΔG_D at 25°C), estimated for the different PAH domains using Eq. (2), are also given in Table 1. Figure 2 shows plots of ΔT_m (T_m of the protein at pH 7.0 – T_m at other pH values) versus pH (a-c) and $\Delta\Delta G_D^o$ (ΔG_D^o of the protein at pH 7.0 – ΔG_D^o at other pH values) versus pH (d-f). As evident from this figure, lowering the pH does not affect the stability of PAH1 but decreases the stability of PAH2 and PAH3 in terms of T_m and ΔG_D^o.

We then investigated the structural variations of the different PAH domains and evaluated how the native-state structural integrity is altered due to change in the pH. For this, we first measured far UV CD (secondary structure) of each of the PAH domains of hSin3B at different pH values (pH 6.3, 6.5, 6.8, and 7.0). It is seen in Fig. 3 that there is a decrease in the secondary structure of PAH2 and PAH3 in a pH-dependent manner, while the structure of PAH1 is not significantly affected by change

Table 1. Thermodynamic parameters of the PAH domains at different pH values

pH	pH 7.0			pH 6.8			pH 6.5			pH 6.3			
Proteins	T_m	ΔH_m	ΔG_D°	T_m	ΔH_m	ΔG_D°	T_m	ΔH_m	ΔG_D°	T_m	H_m	ΔG_D°	ΔC_p
PAH1	65.7	140	12.9	65.3	133	12.0	65.5	136	12.4	65.2	131	11.7	1.53*
PAH2	64.0	119	10.2	62.2	116	9.6	60.3	113	9.0	57.5	109	8.2	1.53
PAH3	63.7	117	9.9	61.8	113	9.2	60.5	111	8.8	58.0	108	8.1	1.54

Notes: The units of T_m, H_m, ΔG_D^o, and ΔC_p are °C, kcal/mol, kcal/mol, and kcal/mol, respectively. Errors in T_m, H_m, ΔG_D^o, and ΔC_p are 0.2-1, 3-6, 7-9, and 5-7%, respectively.

* The value has not been experimentally measured but based on presumptions.

in pH. Figure 4 (a-c) shows the effect of the pH on the tertiary structure of the different PAH domains in terms of the environment of tyrosine residues. It is also seen in this figure that there is an increase in the relative fluorescence intensity in the case of PAH2 and PAH3. However, there is no significant change in the relative fluorescence of PAH1 due to low pH. However, note that the peak maxima was at ~345 nm, which is the ideal peak for tryptophan, and not at ~310 nm, which should be the characteristic emission peak for tyrosine. None of the PAH domains have any tryptophan residues based on our sequencing report and other sequence information available in PubMed. Therefore, the observed peak at ~345 nm purely originates from tyrosine. Previous reports suggest that many proteins that lack tryptophan but have only tyrosine(s) exhibit peak maxima at ~345 nm due to the formation of tyrosinates (the conjugate phenolic base of tyrosine). Tyrosinates are likely formed via an intermolecular proton transfer from the excited state of one or more tyrosine residues to a suitable proton acceptor in the polypeptide. Aspartic and glutamic acid residues are the appropriate proton acceptors [20-23]. PAH1 and PAH3 have only one tyrosine residue, whereas PAH2 has two tyrosine residues. Interestingly, all tyrosine residues observed in the respective polypeptide sequence have either an adjacent or nearby aspartate residue. Figure 4 (d-f) clearly shows that the PAH1 and PAH3 domains do not bind to ANS, as evident from no significant increase in ANS fluorescence intensity and shift in λ_{max}. However, PAH2 shows increase in relative ANS fluorescence but no shift in the λ_{max}, indicating that there may be subtle binding of ANS. These results indicate that the different PAH domains have conformational variations.

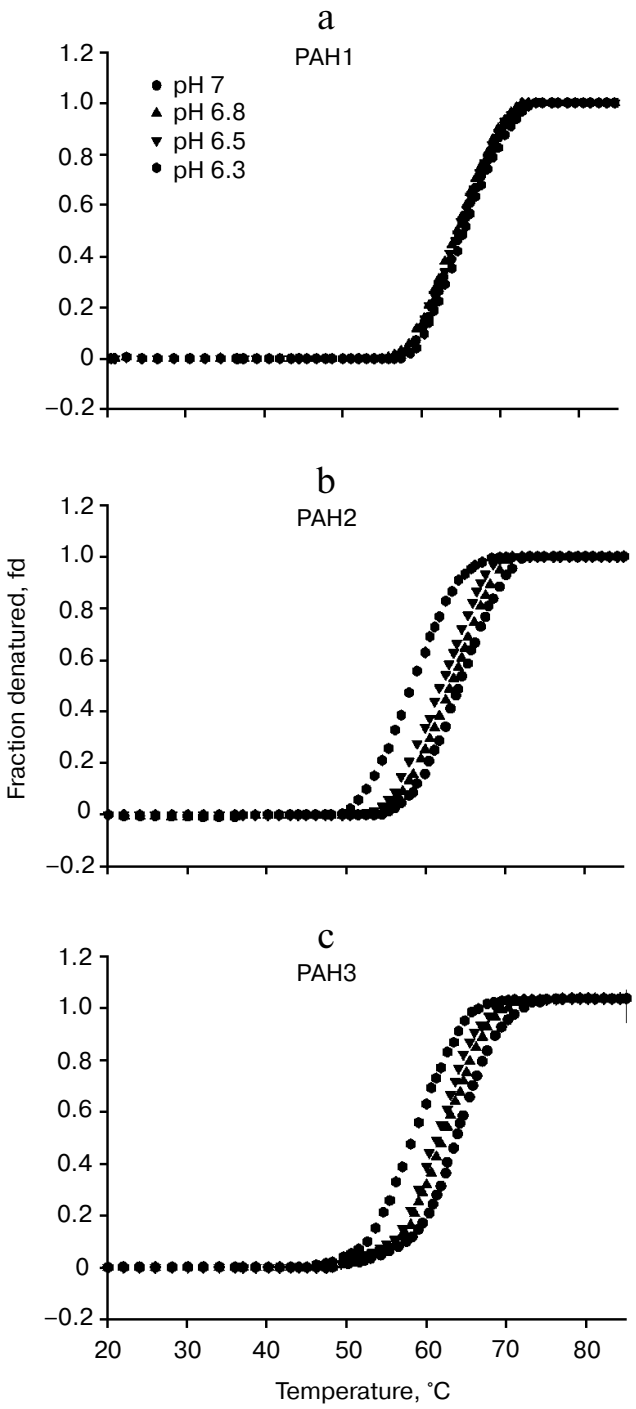

Fig. 1. Heat induced denaturation profile of PAH1 (a), PAH2 (b), and PAH3 (c) at different pH values as indicated in the figure.

DISCUSSION

We have investigated the difference in the thermodynamic stability and structural variations of the different PAH domains of hSin3B and how alteration in pH affect the PAH domains. Thermodynamic stabilities of the three PAH domains were determined by measuring the heat-induced denaturation of the proteins, for which change in θ_{222}, was monitored. At a given pH, ΔG^{o}_{D} was estimated using Eq. (2) with known values of ΔH_m, T_m, and ΔC_p. However, this estimation requires a large extrapolation. Hence, a large error may be associated with ΔG^{o}_{D} determination due to errors in the estimations of ΔH_m, T_m, and ΔC_p. We used Becktel and Schellman's procedure [24] to determine the maximum and minimum errors associated with the ΔG^{o}_{D} determination at a given solvent condition. This procedure involves the estimation of ΔG^{o}_{D} of proteins using the maximum and minimum fitting parameter errors of ΔH_m and ΔC_p (one with maximum error in ΔH_m and minimum error in ΔC_p and the other with minimum error in ΔH_m and maximum error in ΔC_p) obtained from the analysis of individual denaturation curves to yield two different ΔG^{o}_{D} values (one minimum and one maximum). Because there were three independent measurements of ΔH_m and T_m of a protein at the given pH, we obtained six values of ΔG^{o}_{D} (three maximum and three minimum values). All of these six values were used

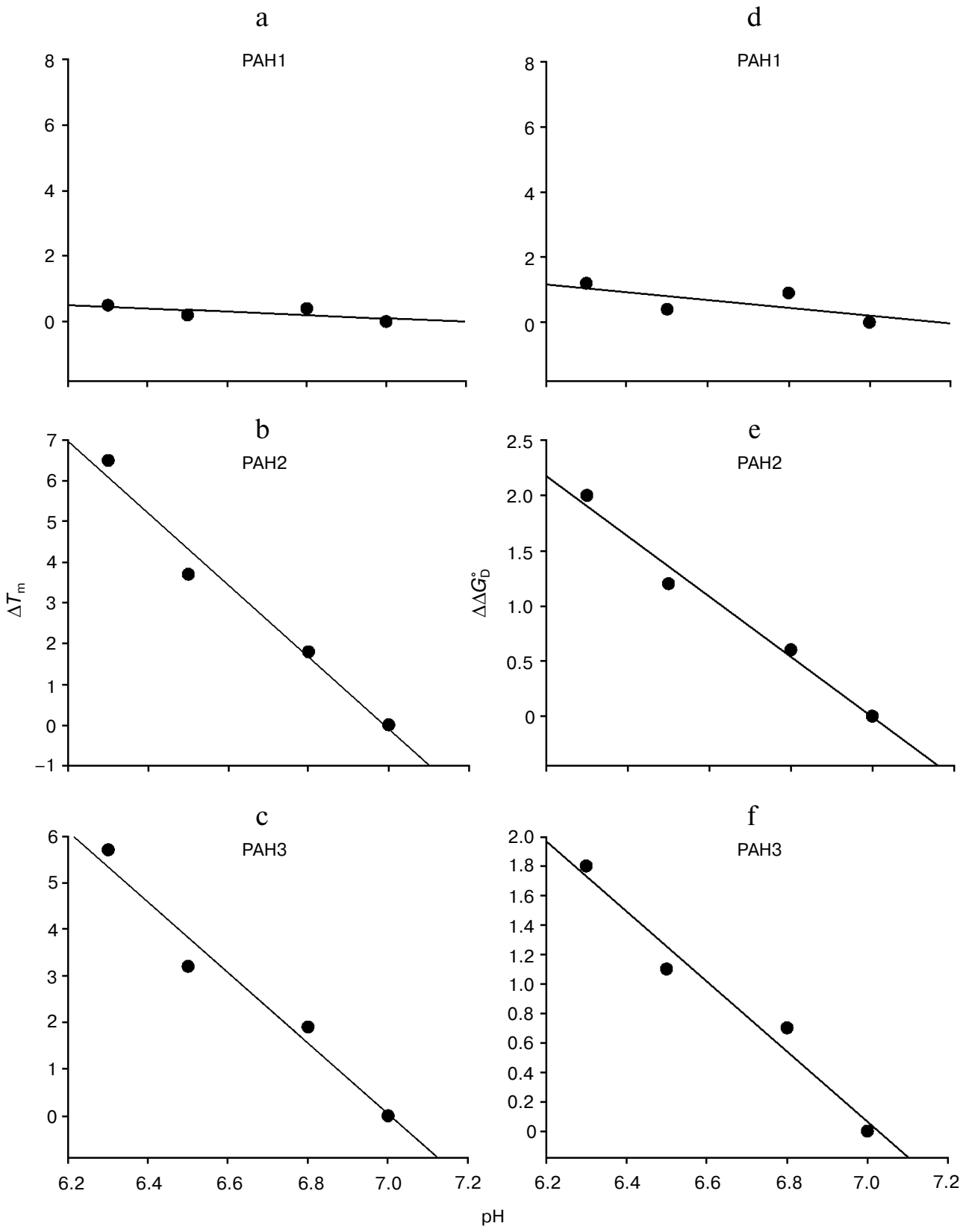

Fig. 2. pH dependence of protein stability. Plots of ΔT_m versus pH (a-c) and $\Delta\Delta G^o_D$ versus pH (d-f) of PAH1, PAH2, and PAH3 at pH 7.0, 6.8, 6.5, and 6.3.

to determine the average ΔG_D^o and the mean error. It was observed that the mean error associated with the ΔG_D^o estimation was in the range 7-9% for all the proteins.

It is seen in Table 1 that PAH1 is more stable than PAH2 and PAH3 at physiological pH in terms of T_m and ΔG_D^o of the proteins. However, it appears that the protein stability for each of the PAH domains is different at physiological and nuclear pH values since the T_m and ΔG_D^o values are different at pH 7.0 and lower pH values (Table 1) indicating that change in pH might regulate the structure and stability of the PAH domains. Therefore, we investigated the effect of different pH values on the PAH domains. For this, we plotted ΔT_m versus pH and $\Delta\Delta G_D^o$ versus pH (Fig. 2). As shown in this figure, for both PAH2 and PAH3 there is a linear relation between the protein stability and pH (in terms of ΔT_m or $\Delta\Delta G_D^o$), i.e. protein stability decreases with decrease in pH. However, the stability of PAH1 does not depend on pH. Thus, protein stability is not always a function of pH for the three PAH domains. The decrease in protein stability due to low pH in the case of PAH2 and PAH3 might mean that the structure should also be destabilized. To investigate this possibility, we measured secondary and tertiary structures of the proteins using far UV CD (Fig. 3) and tyrosine fluorescence (Fig. 4, a-c) as probes, respectively. It is seen in the figures that both the secondary and tertiary structures of PAH2 and PAH3 decrease on lowering pH. As expected, the structure of the PAH1 is not at all perturbed by change in pH. Thus, our thermodynamic and structural measurements are in agreement. The result clearly indicates that change in pH might help to regulate the function of hSin3B. In support to our conclusion, the presence of Sin3 has been reported not only in the nucleus, but also in cytoplasm and mitochondria [25-29]. In addition, there is different partitioning of hSin3B in both the nuclear and cytoplasmic compartments (unpublished results) under stress conditions. It has also been reported that difference in the pH of nucleus and cytoplasm also plays a role in intracellular localization and movement of various proteins between the nuclear and cytoplasmic compartments [30]. Therefore, structural and functional regulation of proteins by change in pH might be a general strategy for many proteins in cells.

Sin3B is a nuclear protein and therefore it is important to compare the structure and stability of the different PAH domains at each of nuclear pH value. ΔG_D^o values given in Table 1 at different nuclear pH values suggest that PAH1 is more stable than PAH2 and PAH3. Interestingly, the stability of both PAH2 and PAH3 are nearly identical at each of the nuclear pH values. We further investigated if the similarity in the thermodynamic stability results in similar structural properties in case of PAH2 and PAH3. Table 2 shows the structural comparison of the three PAH domains under nuclear pH conditions. It is seen in this table that the extent of decrease in secondary structure is higher for PAH2 than for PAH3, while there is no significant change in the secondary structure of PAH1 due to low pH. In agreement with this result, the tertiary structure of PAH2 (based on the relative tyrosine fluorescence) is also a little more disordered relative to PAH3, while the tertiary structure of PAH1 remains unaffected by change in pH. Thus, results on secondary and tertiary measure-

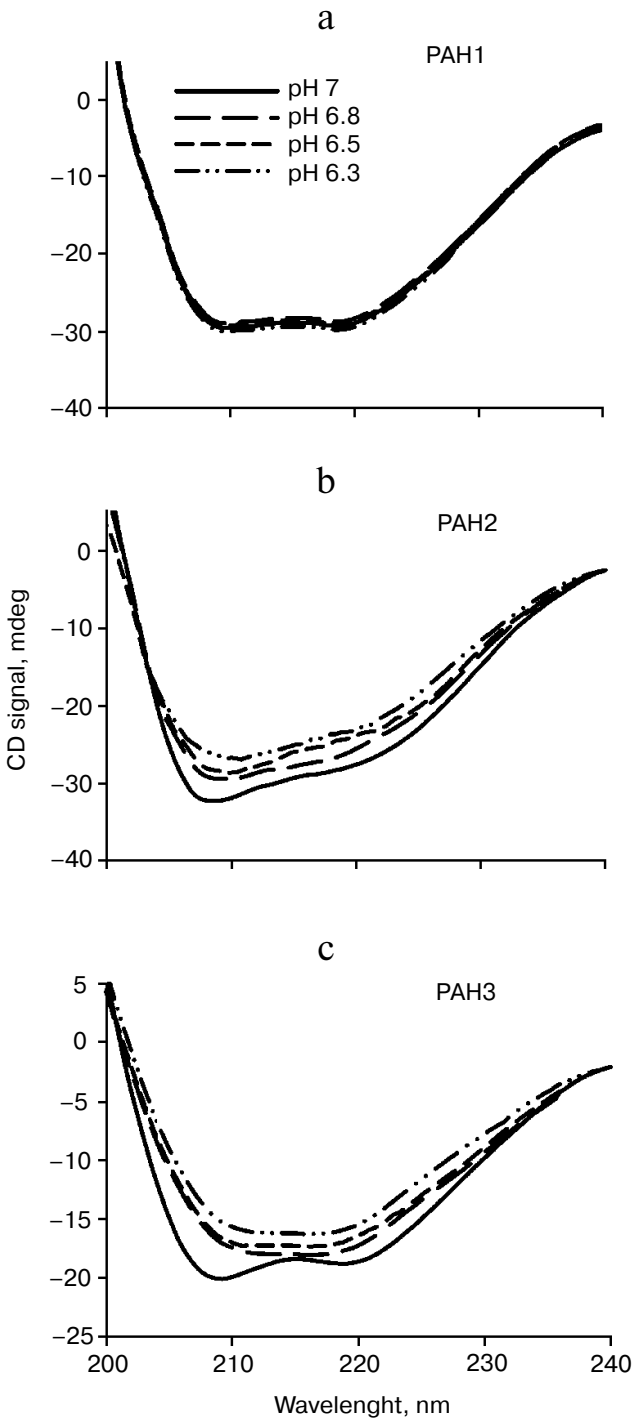

Fig. 3. Effect of pH on the secondary structures of different PAH domains. Far-UV CD spectra (at 37°C) of PAH1 (a), PAH2 (b), and PAH3 (c) incubated overnight at the respective pH values (indicated in the figure).

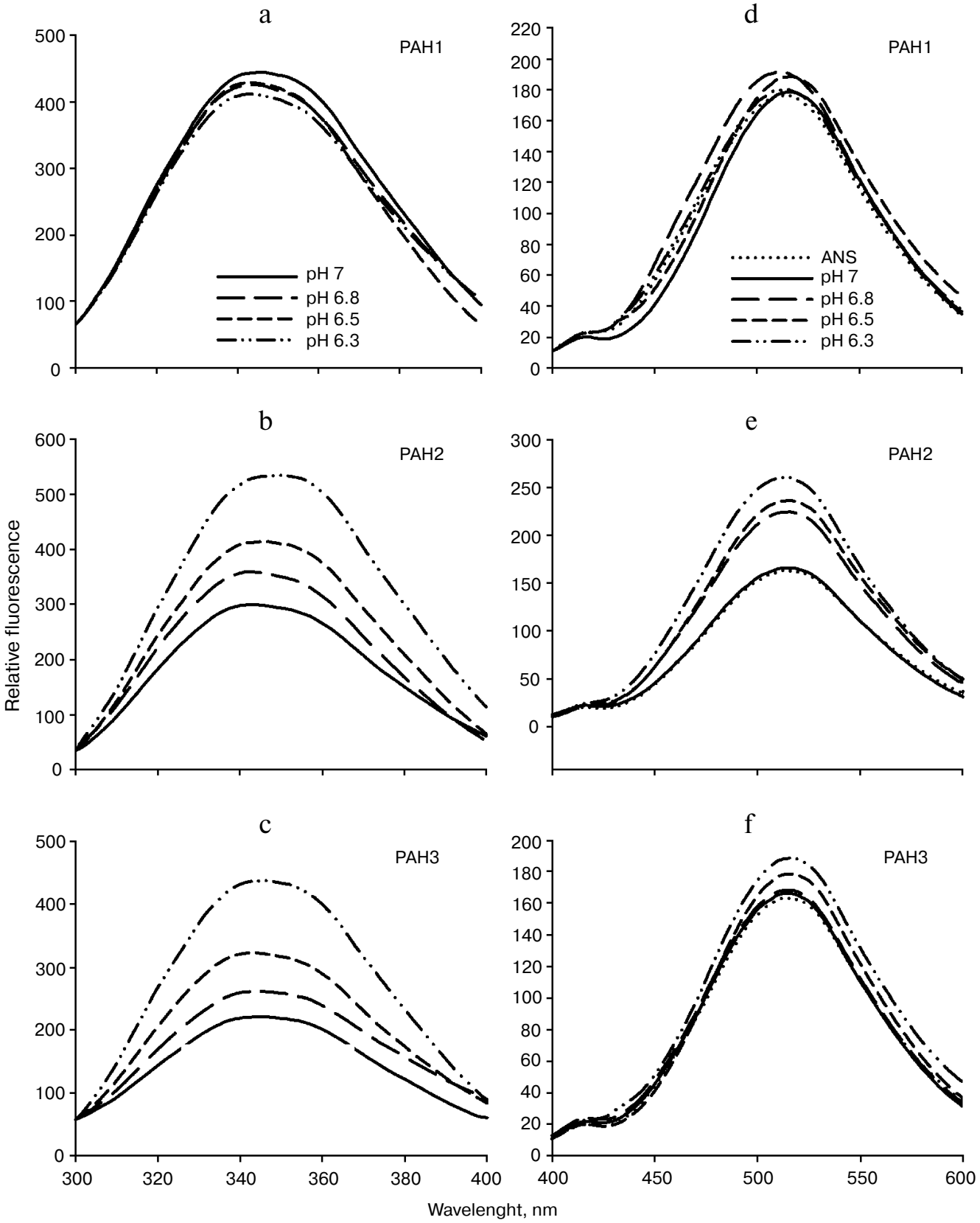

Fig. 4. Effect of pH on the tertiary structure of PAH domains. Intrinsic fluorescence spectra (a-c) and ANS fluorescence spectra (d-f) of PAH1, PAH2, and PAH3.

Table 2. Effect of pH on the structure of PAH domains of human Sin3B (hSin3B)

pH	pH 6.8			pH 6.5			pH 6.3		
Protein	% change (θ_{222})	% change (relative fluorescence)	% change in ANS binding	% change (θ_{222})	% change (relative fluorescence)	% change in ANS binding	% change (θ_{222})	% change (relative fluorescence)	% change in ANS binding
PAH1	2.3	4.4	8.1	1.1	3.9	6.7	1.6	7.8	2.1
PAH2	10	21	38	14	46	45	20	100	60
PAH3	9	17	2.9	11	37	9	18	96	15

Note: Percentage change in θ_{222}, relative fluorescence change, and ANS binding has been evaluated relative to the observed intensities at physiological pH.

ments indicate that there is subtle variation in the structure of the PAH domains. It has been reported that destabilization of the tertiary structure results in the exposure of hydrophobic clusters (that were buried in the interior) to the solvent [20]. We further examined the presence of hydrophobic clusters using ANS binding assay. As evident from Table 2, there is no binding of ANS to PAH1 and PAH3. However, in the case of PAH2 we observed an increase in ANS fluorescence intensity without having a shift in emission maxima, apparently indicating poor binding. All these data led us to believe that the conformation of the different PAH domains at each nuclear pH are different. PAH1 appears to have a very stable native structure, which with subtle variation in pH does not influence its structural integrity, while PAH2 and PAH3 might have relatively flexible structure. It was reported earlier that the structural flexibility and orientation of the PAH domains in case of mammalian Sin3B is crucial for having different binding partners for each of the PAH domains [5, 14, 15, 31]. Interestingly, human PAH1 that is conformationally stable (relative to PAH2 or PAH3) has so far been reported to have only one binding partner – HCF-1. Other than human, in lower organisms only two binding partners have been reported so far for PAH1, SMRTER in *S. cerevisiae* and Opi1 in *Drosophila* [31]. Thus, it seems that the evolutionarily lower conformational flexibility has restrained PAH1 not to interact with a large pool of transcription factors. Human PAH2 and PAH3 that are relatively flexible in structure have been reported to have a large number of binding partners [13]. Taken together, the results indicate that the difference in the conformation of native structure or flexibility of the different PAH domains could result in the recognition of different sets of binding partners.

In conclusion, our studies indicate at least two things: (i) the native state structures and stability of the different PAH domains is different at nuclear pH where Sin3 functions; (ii) PAH2 and PAH3 behave differently at both nuclear and physiological pH in terms of native state structure and stability, while the structure of PAH1 remains unaltered at both pH values. The study indicates the importance of structural heterogeneity in PAH domains in recruiting or recognizing a specific set of binding partners. Further research should focus on identifying the functional importance of PAH1 in hSin3B, as it represents a highly stable native structure.

This work was supported by grant from the Council of Scientific and Industrial Research (File No. 37 (1596/13/EMR-II)). L.R.S. and T.H. acknowledge Indian Council for Medical Research for the financial assistance provided in the form of research fellowship (File No. 3/1/3/JRF-2010/MBD-2 (33050)).

REFERENCES

1. Grzenda, A., Lomberk, G., Zhang, J.-S., and Urrutia, R. (2009) Sin3: master scaffold and transcriptional corepressor, *Biochim. Biophys. Acta (BBA)-Gene Regul. Mechanisms*, **1789**, 443-450.
2. Kadamb, R., Mittal, S., Bansal, N., Batra, H., and Saluja, D. (2013) Sin3: insight into its transcription regulatory functions, *Europ. J. Cell Biol.*, **92**, 237-246.
3. McDonel, P., Costello, I., and Hendrich, B. (2009) Keeping things quiet: roles of NuRD and Sin3 co-repressor complexes during mammalian development, *Int. J. Biochem. Cell Biol.*, **41**, 108-116.
4. Hassig, C. A., Fleischer, T. C., Billin, A. N., Schreiber, S. L., and Ayer, D. E. (1997) Histone deacetylase activity is required for full transcriptional repression by mSin3A, *Cell*, **89**, 341-347.
5. Le Guezennec, X., Vermeulen, M., and Stunnenberg, H. G. (2006) Molecular characterization of Sin3 PAH-domain interactor specificity and identification of PAH partners, *Nucleic Acids Res.*, **34**, 3929-3937.
6. Sahu, S. C., Swanson, K. A., Kang, R. S., Huang, K., Brubaker, K., Ratcliff, K., and Radhakrishnan, I. (2008)

Conserved themes in target recognition by the PAH1 and PAH2 domains of the Sin3 transcriptional corepressor, *J. Mol. Biol.*, **375**, 1444-1456.
7. Ayer, D. E., Lawrence, Q. A., and Eisenman, R. N. (1995) Mad-Max transcriptional repression is mediated by ternary complex formation with mammalian homologs of yeast repressor Sin3, *Cell*, **80**, 767-776.
8. Yang, Q., Kong, Y., Rothermel, B., Garry, D. J., Bassel-Duby, R., and Williams, R. S. (2000) The winged-helix/forkhead protein myocyte nuclear factor beta (MNF-beta) forms a co-repressor complex with mammalian sin3B, *Biochem. J.*, **345**, 335-343.
9. Alland, L., Muhle, R., Hou, H., Potes, J., Chin, L., Schreiber-Agus, N., and DePinho, R. A. (1997) Role for N-CoR and histone deacetylase in Sin3-mediated transcriptional repression, *Nature*, **387**, 49-55.
10. Rayman, J. B., Takahashi, Y., Indjeian, V. B., Dannenberg, J.-H., Catchpole, S., Watson, R. J., te Riele, H., and Dynlacht, B. D. (2002) E2F mediates cell cycle-dependent transcriptional repression *in vivo* by recruitment of an HDAC1/mSin3B corepressor complex, *Genes Devel.*, **16**, 933-947.
11. Spronk, C. A. E. M., Tessari, M., Kaan, A. M., Jansen, J. F. A., Vermeulen, M., Stunnenberg, H. G., and Vuister, G. W. (2000) The Mad1-Sin3B interaction involves a novel helical fold, *Nature Struct. Mol. Biol.*, **7**, 1100-1104.
12. Olsson, A., Olsson, I., and Dhanda, R. S. (2008) Transcriptional repression by leukemia-associated ETO family members can be independent of oligomerization and coexpressed hSIN3B and N-CoR, *Biochim. Biophys. Acta (BBA)-Gene Regul. Mechanisms*, **1779**, 590-598.
13. Silverstein, R. A., and Ekwall, K. (2005) Sin3: a flexible regulator of global gene expression and genome stability, *Curr. Genet.*, **47**, 1-17.
14. Van Ingen, H., Baltussen, M. A. H., Aelen, J., and Vuister, G. W. (2006) Role of structural and dynamical plasticity in Sin3: the free PAH2 domain is a folded module in mSin3B, *J. Mol. Biol.*, **358**, 485-497.
15. Swanson, K. A., Knoepfler, P. S., Huang, K., Kang, R. S., Cowley, S. M., Laherty, C. D., Eisenman, R. N., and Radhakrishnan, I. (2004) HBP1 and Mad1 repressors bind the Sin3 corepressor PAH2 domain with opposite helical orientations, *Nature Struct. Mol. Biol.*, **11**, 738-746.
16. Kumar, G. S., Xie, T., Zhang, Y., and Radhakrishnan, I. (2011) Solution structure of the mSin3A PAH2–Pf1 SID1 complex: a Mad1/Mxd1-like interaction disrupted by MRG15 in the Rpd3S/Sin3S complex, *J. Mol. Biol.*, **408**, 987-1000.
17. Van Ingen, H., Lasonder, E., Jansen, J. F. A., Kaan, A. M., Spronk, C. A. E. M., Stunnenberg, H. G., and Vuister, G. W. (2004) Extension of the binding motif of the Sin3 interacting domain of the Mad family proteins, *Biochemistry*, **43**, 46-54.
18. Saluta, M., and Bell, P. A. (1998) Troubleshooting GST fusion protein expression in *E. coli*, *Life Sci. News*, **1**.
19. Marty, A., Boiret, M., and Deumie, M. (1986) How to illustrate ligand–protein binding in a class experiment: an elementary fluorescent assay, *J. Chem. Ed.*, **63**, 365.
20. Lakowicz, J. R. (2007) *Principles of Fluorescence Spectroscopy*, Springer.
21. Szabo, A. G., Lynn, K., Krajcarski, D., and Rayner, D. M. (1979) Tyrosine fluorescence at 345 nm in proteins lacking tryptophan, *J. Luminesc.*, **18**, 582-586.
22. Szabo, A. G., Lynn, K. R., Krajcarski, D. T., and Rayner, D. M. (1978) Tyrosinate fluorescence maxima at 345 nm in proteins lacking tryptophan at pH 7, *FEBS Lett.*, **94**, 249-252.
23. Ruan, K., Li, J., Liang, R., Xu, C., Yu, Y., Lange, R., and Balny, C. (2002) A rare protein fluorescence behavior where the emission is dominated by tyrosine: case of the 33-kDa protein from spinach photosystem II. *Biochem. Biophys. Res. Commun.*, **293**, 593-597.
24. Becktel, W. J., and Schellman, J. A. (1987) Protein stability curves, *Biopolymers*, **26**, 1859-1877.
25. Barnes, V. L., Strunk, B. S., Lee, I., Huttemann, M., and Pile, L. A. (2010) Loss of the SIN3 transcriptional corepressor results in aberrant mitochondrial function, *BMC Biochem.*, **11**, 26.
26. Backues, S. K., Lynch-Day, M. A., and Klionsky, D. J. (2012) The Ume6-Sin3-Rpd3 complex regulates ATG8 transcription to control autophagosome size, *Autophagy*, **8**, 1835-1836.
27. Kong, Q., Zeng, W., Wu, J., Hu, W., Li, C., and Mao, B. (2010) RNF220, an E3 ubiquitin ligase that targets Sin3B for ubiquitination, *Biochem. Biophys. Res. Commun.*, **393**, 708-713.
28. Khochbin, S., Verdel, A., Lemercier, C., and Seigneurin-Berny, D. (2001) Functional significance of histone deacetylase diversity, *Curr. Opin. Genet. Devel.*, **11**, 162-166.
29. Vega, A. V., Avila, G., and Matthews, G. (2013) Interaction between the transcriptional corepressor Sin3B and voltage-gated sodium channels modulates functional channel expression, *Sci. Rep.*, **3**.
30. Cunningham, J., Estrella, V., Lloyd, M., Gillies, R., Frieden, B. R., and Gatenby, R. (2012) Intracellular electric field and pH optimize protein localization and movement, *PloS One*, **7**, e36894.
31. Nomura, M., Uda-Tochio, H., Murai, K., Mori, N., and Nishimura, Y. (2005) The neural repressor NRSF/REST binds the PAH1 domain of the Sin3 corepressor by using its distinct short hydrophobic helix, *J. Mol. Biol.*, **354**, 903-915.